Seasonal siderophore uptake and biosynthesis associated with carbon flux at Station ALOHA

Randelle M. Bundy[1,*] and Lauren E. Manck[2,*], Rene M. Boiteau[3], Jiwoon Park[1], Edward F. DeLong[4], Nicholas J. Hawco[4], Matthew J. Church[2], Mak A. Saito[5], Daniel J. Repeta[5]

[1]University of Washington, School of Oceanography, Seattle, WA
[2]University of Montana, Flathead Lake Biological Station, Polson, MT
[3]Oregon State University, College of Earth Ocean and Atmospheric Sciences, Corvallis, OR
[4]University of Hawaii at Manoa, Center for Microbial Oceanography Research and Education, Honolulu, HI
[5]Woods Hole Oceanographic Institution, Marine Chemistry and Geochemistry, Woods Hole, MA

[*]co-first authors and corresponding authors rbundy@uw.edu and lauren.manck@flbs.umt.edu

Running head (40 characters): Siderophore biosynthesis at Station ALOHA

Author contribution statement: RBundy and LEM wrote the manuscript and completed the analyses. RBoiteau and JP contributed data and edited the manuscript. EFD, MJC, MAS and DJR helped design the study and edit the manuscript.

Scientific Significance Statement (125 words; including a setup, challenge, and resolution- currently 114 words**)**

Microbial community production in the subtropical oligotrophic North Pacific is limited by macronutrients such as nitrogen and phosphorous. However, dissolved iron is another important micronutrient that has seasonal inputs from dust and passing eddies, keeping the availability of iron low and episodic. Little attention has been paid to the microbial strategies for dealing with low iron to support primary production in the oligotrophic ocean, or how limited iron availability impacts the processing of sinking particulate organic carbon in this region. In this study, we explore siderophore production and uptake throughout the water column at Station ALOHA to examine how the microbial community adapts and responds to changing iron and carbon availability on seasonal timescales.

Abstract (**150 words**- currently 150 words)

Dissolved iron concentrations in the North Pacific subtropical oligotrophic gyre are low, in part due to biological consumption and seasonally restricted iron delivery to these waters. In this study, we examined seasonal changes in dissolved siderophore concentrations, uptake rates and biosynthesis at Station ALOHA to observe changes in iron acquisition by the microbial community. Genetic potential for siderophore biosynthesis was widespread throughout the upper water column (0-500 m) and peaked in spring and summer along with siderophore concentrations. Uptake rates were faster and residence times of siderophore-bound iron were shorter at 300 m compared to 15 m, suggesting differences in iron acquisition in the mesopelagic. Changes in siderophore production in the water column suggest that variations in primary production and carbon export impact iron acquisition of the microbial community over the seasonal cycle and provides initial evidence that iron demand may change in association with carbon export at Station ALOHA.

Keywords: siderophore, dissolved iron, siderophore biosynthesis, Station ALOHA

Data Availability Statement: Iron uptake data are available as supplementary files and on Zenodo (DOI: 10.5281/zenodo.7062571). Sequence data are available from the NCBI short read archive (SRA) under Bioproject no. PRJNA352737.

(Main body- 3,000 words- currently 3,598 words including references; 3,345 without references**)**

1. Introduction

Oligotrophic subtropical gyres comprise the world's largest ocean biome (Longhurst 2010). Microbial communities inhabiting the oligotrophic ocean are exposed to low concentrations of nitrogen and phosphorous (Karl et al. 1997; Fitzsimmons and Boyle 2014; Letelier et al. 2019), and dissolved iron (Fitzsimmons et al. 2015). The Hawaii Ocean Time-series (HOT) at Station ALOHA in the North Pacific subtropical gyre is one of the longest running open ocean time-series programs, and observations from the HOT program study site have demonstrated how seasonal changes in nutrient supply impact the microbial community and carbon export (Karl and Lukas 1996). The resulting time series captures both the relatively stable conditions of the oligotrophic ocean and the importance of episodic and seasonal-scale delivery of nutrients to the upper ocean from passing eddies, seasonal dust inputs, and the shoaling and deepening of the pycnocline (Fitzsimmons et al. 2015; Hayes et al. 2015; Pinedo-González et al. 2020).

Seasonal changes in the external supply of iron to Station ALOHA impacts microbial community composition and can trigger organic ligand production on the timescale of days (Fitzsimmons et al. 2015; Hayes et al. 2015). Some of the strongest organic iron-binding ligands called siderophores are produced by marine bacteria and fungi and can alter the bioavailability and recycling of dissolved iron (Sandy and Butler 2009; Vraspir and Butler 2009). Siderophores are synthesized by either a non-ribosomal peptide synthetase (NRPS) pathway or an NRPS-independent siderophore (NIS) synthetase pathway and are secreted into the marine environment to facilitate the uptake of iron (Sandy and Butler 2009; Hider and Kong 2010). Siderophore biosynthesis is regulated by iron concentrations, where elevated concentrations of iron suppress synthesis (Sandy and Butler 2009). Some microbes possess the genetic potential for both synthesizing and internalizing siderophores, while others "cheat" and only possess outer membrane receptors for exogenous siderophore uptake (Cordero et al. 2012; Kramer et al. 2020). Internalizing siderophore-bound iron requires either specific transport pathways or the ability to reduce Fe(III) to Fe(II) from the siderophore complex; thus iron complexed to siderophores has low bioavailability to the microbial community as whole (Shaked and Lis 2012). Although dissolved siderophores represent from 2-10% of the total dissolved iron-binding ligand pool at Station ALOHA, they likely play an important role in competition and recycling of iron, and facilitate the solubilization of iron from particles (Bundy et al. 2018).

The potential importance of siderophore production as a microbial iron acquisition strategy has been recognized for some time, but measurements of the distributions of siderophores in seawater are scarce (Mawji et al. 2008a; Boiteau et al. 2016, 2019; Bundy et al. 2018; Moore et al. 2021; Manck et al. 2022) and little is known about the factors that influence their seasonal variability. In this study, we explore seasonal changes in water column siderophore distributions, biosynthesis potential and residence times at Station ALOHA in the context of the HOT program to explore the conditions that impact microbial iron acquisition in this important oligotrophic ecosystem.

2. Methods

2.1 Siderophore sample collection and analyses

Dissolved siderophore samples were collected from six cruises (*n* = 2 winter, *n* = 2 spring, *n* = 1 summer, *n* =1 fall) from 2013-2016. Additional contextual data from three of the six cruises are presented elsewhere (Table S1). Samples were collected via Teflon diaphragm pump or 8 L X-Niskin bottles on a trace metal rosette using a non-metallic line. Samples were filtered (0.2 µm Acropak 200 or Pall capsule filter) into either acid-cleaned fluorinated high density polyethene 200 L barrels (Boiteau et al. 2013) or acid-cleaned 20 L carboys (Bundy et al. 2018). Filtered samples were pumped onto solid phase extraction columns (ENV resin, Agilent Technologies), and stored at -20°C until analysis. Details on sample analysis can be found in Bundy et al. (2018). Putative siderophores were detected using liquid chromatography inductively coupled plasma mass spectrometry (LC-ICP-MS), where chromatographically resolved peaks were quantified. Only iron-bound siderophores were quantified, and putative siderophores were identified based on the alignment of an MS^1 peak with an ^{56}Fe peak in the LC-ICP-MS data and corresponding MS^2 fragments that matched either published literature or *in silico* fragmentation (Supplementary Methods). A siderophore assignment was not possible for all putative siderophores, and in those cases only the total concentration is reported (Table S1). Average dissolved siderophore concentrations were binned by depth and season to match the metagenome sampling resolution.

2.2 Iron uptake and siderophore bioavailability experiments

Iron uptake experiments were performed on two expeditions (HOT278 in November 2015 and KM1605 in March 2016). During the HOT278 expedition, experiments were performed in surface waters (15 m; *n* = 3) and during KM1605 experiments were performed at 15 m and 300 m (*n* = 2). Four treatments were used in all experiments: $FeCl_3$ (denoted as "FeL"), ferrioxamine B, ferrioxamine E, and Fe-amphibactin. Experiments at 15 m were performed both in the light and dark, and experiments at 300 m were only performed in the dark. Iron uptake was measured in the 2.0 µm and 0.2 µm size fraction after 12 hours and multiplied by 2 to calculate an iron uptake rate per day. 500 nmol L^{-1} of nitrate was added to each of the 15 m experiments to control for nitrogen limitation preventing the uptake of iron.

The isolation of the amphibactins used in this experiment have been described in detail elsewhere (Bundy et al. 2018), and other ligand standards were commercially available. Radioactive ^{55}Fe (Perkin Elmer) was added to the amphibactin, desferrioxamine B, and desferrioxamine E ligand stocks and was equilibrated for at least 24 hours before use. Non-radioactive ligand stocks were made with ^{57}Fe (Cambridge Isotopes) to set-up replicate treatments for cell counts without radioactive iron. Trace metal clean unfiltered seawater from 15 m and 300 m was dispensed into 250 mL acid-cleaned polycarbonate bottles. Four of the bottles were spiked with 1 nmol L^{-1} of the ^{57}Fe stocks (one for each treatment) and the rest were spiked in duplicate with 1 nmol L^{-1} of the ^{55}Fe ligand stocks. A final concentration of 0.01% glutaraldehyde was added to four of the bottles as dead controls and were incubated for 30 minutes before the experiment began to account for ^{55}Fe adsorption to particles.

Bottles were incubated in surface seawater flow-through incubators and dark treatments were double-bagged in black polyethylene bags. After 12 hours, each bottle was filtered onto acid washed 2.0 µm and 0.2 µm filters using low pressure vacuum filtration. Both filters were washed three times with an oxalate wash to remove extracellular iron (Tovar-Sanchez 2003).

Radioactive decay for each sample was determined using a liquid scintillation counter (Beckman-Coulter LS6500). ^{55}Fe disintegrations per minute (dpm) were background and dead control corrected and converted to iron uptake using a standard curve. Cell count samples were taken from ^{57}Fe treatments at the beginning and end of each experiment (Supplementary Methods). Iron uptake per cell was estimated based on flow cytometry cell counts of cyanobacteria, photosynthetic picoeukaryotes and heterotrophic bacteria (Table S2), and Fe:C ratios for heterotrophic bacteria were determined only in the dark treatments using heterotrophic bacteria abundances and an estimated carbon per cell of 12.4 fg C cell^{-1} (Boyd et al. 2015). The turnover time of iron in each treatment was calculated by,

(1) $$turnover\ time = {}^{total\ iron\ uptake}/_{total\ iron}$$

where the total iron uptake (pmol L^{-1} day^{-1}) is the sum of the radioactive iron uptake in the 2.0 and 0.2 µm fraction and the total iron is the radioactive iron added (1 nmol L^{-1}) plus the *in situ* dissolved iron. Residence times of iron (days) was calculated as 1/turnover time.

2.3 Genomic sample collection and analyses

Details on the sampling, processing and data analyses of metagenomes collected at Station ALOHA are presented elsewhere (Mende et al. 2017; Luo et al. 2020). The ALOHA gene catalog consists of ~8.9 million non-redundant genes identified at Station ALOHA between the surface and 1,000 m over the course of ~1.5 years collected on 0.2 µm filters (Mende et al. 2017). The ALOHA gene catalog was probed for both NRPS and NIS biosynthetic gene clusters (BGCs) by searching for the conserved domains present within biomarker genes. For NIS pathways, hidden Markov models (HMMs) for the conserved domains pfam04183 (IucA/IucC siderophore synthase) and pfam06276 (FhuF-like reductase) were searched using HMMER (Eddy 2011). For NRPS biosynthetic pathways, the HMM for the conserved domain pfam00501, an AMP-binding domain inclusive of the adenylation domain of NRPS modules, was searched. The resulting 28,000+ genes were then screened with antiSMASH (Medema et al. 2011) to determine the presence of a complete or near- complete NRPS module. The resulting NRPS BGCs were then further examined to determine those specific to siderophore biosynthesis (Supplementary Methods). In total, 38 putative siderophore BGCs were identified and used for downstream analysis (Table S3).

To examine the distribution of siderophore BGCs with depth and time at Station ALOHA, metagenomic reads from samples collected on HOT cruises between May 2015 and April 2016 (n = 132, 5-500 m) (Luo et al. 2020) were mapped to open reading frames (ORFs) of the ALOHA gene catalog using BWA (Li and Durbin 2009), counted with FeatureCounts (Liao et al. 2014), and normalized to reads per kilobase per million (RPKM). Reads from the 2015-2016 dataset recruited to 24 of the 38 siderophore BGCs identified in the ALOHA gene catalog (Table S3).

3. Results

3.1 Seasonal distribution of siderophores and siderophore biosynthesis genes at Station ALOHA

Dissolved siderophore concentrations and the presence of siderophore BGCs changed seasonally at Station ALOHA (Fig. 1A). Average siderophore concentrations were highest in the spring, summer and fall, and were lower in winter, though variability was high (Fig. 1A). Similar patterns were observed in siderophore BGCs from metagenomes (Fig. 1B). The normalized abundance of siderophore BGCs peaked in the spring and summer and were lowest in winter, similar to the concentrations of total dissolved siderophores (Fig. 1C). In the spring, peaks in siderophore BGCs were largely associated with surface waters (Fig. 2A), though subsurface maxima were also observed below the deep chlorophyll maximum (DCM) and the euphotic zone (250 m). Summer maxima in siderophore BGCs were almost exclusively associated with the DCM (Fig. 2B). A similar pattern was observed in the fall, where siderophore BGCs were maximal in the DCM and 175 m (Fig. 2C). The winter showed lower genetic potential for siderophore biosynthesis overall, with median ORF abundances less than 0.2 RPKM at all depths (Fig. 2D). Overall, the highest concentrations of both dissolved siderophores and normalized read counts of siderophore BGCs were observed in the upper euphotic zone (< 75 m), the DCM (75-125 m), and upper mesopelagic (225-300 m).

Several different types of siderophores were characterized in the water column and are capable of being synthesized by the *in situ* microbial community (Table 1). Of those identified in the water column, primarily hydroxamate siderophores were detected, with ferrioxamines and amphibactins being the most common classes (Table 1). The siderophore BGCs identified largely belonged to catecholate and carboxylate-type siderophores (Table 1). Two ferrioxamine BGCs were identified in the gene catalog; however, these BGCs were not detected in the 2015-2016 metagenomic dataset. Amphibactin BGCs, as determined by the presence of a N^5-acyl-N^5-hydroxyornithine NRPS adenylation domain, were not detected. Several siderophores were found both in the water column and as a BGC in the metagenomes, including petrobactin, pseudoalterobactin, piscibactin and vibrioferrin (Table 1). The biosynthesis genes were primarily from the genera *Vibrio*, *Photobacterium*, *Alteromonas*, and *Pseudoalteromonas* (Table S3).

3.4 Uptake and residence time of siderophore-bound iron by the in situ microbial community

Siderophore-bound iron was readily accessible by the microbial community in both the surface (15 m) and upper mesopelagic (300 m) waters at Station ALOHA. Uptake rates of inorganic iron, which was likely associated with unknown natural organic iron-binding ligands (denoted "FeL"), were higher than for siderophore-bound iron (Fig. 3A). The uptake rate of FeL was also higher when the experiment was performed in the light compared to the dark (Fig. 3A). The uptake rate varied for the different iron-siderophore complexes. The iron-amphibactin was taken up the fastest, followed by ferrioxamine E and ferrioxamine B. In contrast to FeL, the uptake rate of siderophore-bound iron was always higher in the dark compared to the light (Fig. 3A). Overall, the total iron uptake was also higher in the 0.2 µm fraction compared to the 2.0 µm fraction in all experiments and treatments (Fig. 3A). Surprisingly, the uptake rate of siderophore-bound iron was higher at 300 m compared to 15 m despite the 3-fold lower cell abundances, leading to high iron uptake per cell (Table S2) and shorter residence times of iron (Fig. 3B). Assuming the total iron uptake in the dark was due to heterotrophic bacteria, the estimated Fe:C (µmol:mol) of the heterotrophic bacteria community in surface waters ranged from 6.8-68 µmol:mol while at 300 m they ranged from 88-710 µmol:mol (Table S2). The average residence time of iron was shorter at 300 m compared to 15 m (Fig. 3B), though this difference was only

significant in the DFB treatment (pairwise t-test, $p < 0.05$). The average residence time of iron at 15 m ranged from 15 days in the FeL treatment to 252 and 215 days in the DFE and DFB treatments, respectively. The average residence times at 300 m ranged from 9 days in the FeL treatment to 65 days in the DFB treatment.

4. Discussion

4.1 Siderophore production and uptake at Station ALOHA

Siderophore BGCs and measurements of dissolved siderophores highlight seasonal differences in microbial iron acquisition at Station ALOHA (Fig. 1 and 2). Both siderophore concentrations and biosynthesis potential were greatest in the spring, summer and fall and were almost entirely absent in winter. Although our data do not capture instantaneous siderophore production by bacteria, it is likely that siderophore secretion is being used to solubilize particulate iron (Bundy et al. 2018) and to compete with other organisms for iron (Boiteau et al. 2016). Several genera found to have siderophore BGCs, such as *Vibrio* and *Alteromonas*, contain known copiotrophic bacteria, suggesting that siderophore production may be common to heterotrophs that are opportunistic and respond to episodic inputs of nutrients or carbon during the spring and summer (Fontanez et al. 2015; Pelve et al. 2017; Church et al. 2021; Poff et al. 2021; Leu et al. 2022). Interestingly, there was little overlap in the dominant siderophores measured and the BGCs identified (Table 1). The siderophore BGCs were primarily catecholates, while those measured in the water column were primarily hydroxamates. This implies that catecholate siderophores could be below our detection limits, or rapidly cycled in the water column. Conversely, the structural discrepancy between siderophores detected in BGCs and those dominating water column measurements at Station ALOHA and in other regions (Mawji et al. 2008b; Boiteau et al. 2016; Bundy et al. 2018), suggests that the importance of these compounds may be underestimated by metagenomic studies.

Microbial iron recycling via the production and consumption of siderophore-bound iron likely involves rapid turnover of these compounds. The iron uptake experiments conducted here provided estimates of the residence time of weakly bound (FeL) versus siderophore-bound iron. Siderophore-bound iron was taken up less rapidly by the microbial community and had average residence times ranging from 15-250 days (Fig. 3A), while FeL was highly labile and had average residence times of 1-2 weeks (Fig. 3B). The FeL treatment likely had a short residence time since inorganic iron may associate with weaker ligands when added to seawater, which are more accessible to phytoplankton using ferric reductases as an uptake mechanism (Maldonado and Price 2001; Salmon et al. 2006; Lis et al. 2015; Coale et al. 2019). Iron uptake rates in FeL treatments were higher in the light than in the dark, suggesting significant contributions by photoautotrophs. Uptake rates of siderophore-bound iron in contrast were always higher in the dark than the light, suggesting no significant photochemical effect on the uptake rate of siderophores (Barbeau 2006), and that siderophore iron consumption was likely not controlled by photosynthetic plankton.

The siderophore treatments had slower uptake rates and longer residence times than FeL. Iron associated with amphibactins was taken up more quickly than ferrioxamine E or B (Fig. 3A). Amphibactins have a lower binding affinity to dissolved iron (stability constants = 12.0-12.5)

compared to ferrioxamines (14.0-14.4; (Bundy et al. 2018)), and iron is likely more easily reducible from amphibactins. Alternatively, more members of the microbial community may possess Fe-amphibactin uptake pathways. Siderophore-bound iron also appeared to be more rapidly internalized by heterotrophic bacteria compared to large photoautotrophs at Station ALOHA. Iron uptake in the 0.2 µm size fraction was assumed to be dominated by free-living bacteria, and the total iron uptake in this fraction was always greater than the 2.0 µm (Fig. 3A). An unexpected result was the faster uptake rates and shorter residence times of siderophore-bound iron at 300 m compared to 15 m. Macronutrient concentrations are elevated at 300 m relative to 15 m, so it is possible iron uptake rates were enhanced due to relief from macronutrient limitation. However, nitrogen amendments (500 nmol L^{-1}) to the surface community should have alleviated nitrogen limitation. The experiments at 300 m were also incubated at the same temperature as the 15 m experiments, likely enhancing the uptake rate of iron relative to *in situ* rates, however it is not clear why this would stimulate uptake rates above those measured in surface waters.

Fast uptake rates and short residence times of iron at 300 m are likely related to differences in iron acquisition by the microbial community at these depths. The iron requirements of heterotrophic bacteria are not well known, but evidence suggests they are elevated relative to large phytoplankton (Fe:C ~ 2.0 µmol: mol) or cyanobacteria (Fe:C ~ 19 µmol: mol) (Strzepek et al. 2005). Published estimates for heterotrophic bacteria Fe:C range from 7.5 µmol: mol (Tortell et al. 1996) to 83 µmol: mol (Mazzotta et al. 2020). Our range in Fe:C in surface waters encompass these values, but exceed this range at 300 m (Table S2). One explanation is the carbon per cell estimates for heterotrophic bacteria are not representative of upper mesopelagic bacteria, causing the Fe:C to be high. Nitrifiers for example, have both high carbon (Watson and Mandel 1971) and iron content (Saito et al. 2020). Alternatively, the microbial community at these depths could have elevated iron requirements, as the electron transport systems used for respiration is iron-intensive (Tortell et al. 1996) and changes in the lability or oxidation state of organic matter might impact iron demand. The community at 300 m may also be exposed to elevated iron in the form of particulate iron throughout the season, and may engage in luxury uptake and storage (Mazzotta et al. 2020). The high iron uptake rates per cell led to shorter residence times at 300 m, particularly for siderophore-bound iron (Fig. 3B) consistent with the shorter residence times observed in the DCM in other studies (Hawco et al. 2022). Siderophore turnover may be particularly fast in the mesopelagic as bacteria recycle and regenerate iron from sinking particles (Bundy et al. 2018). The reason for the enhanced iron uptake at 300 m is unknown, but understanding the iron demands of mesopelagic bacteria could have important implications for carbon and iron cycling in the mesopelagic.

4.2 Environmental drivers of siderophore production and consumption

Seasonality in productivity, particle accumulation, iron supply and export have all been documented at Station ALOHA (Fitzsimmons et al. 2015; Hawco et al. 2021; Karl et al. 2021) and such changes likely impact microbial siderophore production. As productivity increases in the late spring in the gyre, dissolved iron concentrations are drawn down and competition for iron intensifies (Fitzsimmons et al. 2015), setting up conditions that likely favor the production of siderophores to recycle and retain iron in the euphotic zone (Boyd et al. 2015; Hawco et al. 2022). In the summer as carbon export fluxes increase, dissolved siderophore concentrations

increased deeper in the water column and the siderophore BGCs peaked closer to the DCM (Fig 1A, 2B). This could reflect further competition and recycling of iron later in the growing season, including greater overall iron demand by the heterotrophic bacteria community to process particulate organic matter. There could also be a shift in the microbial community at depth to reflect more siderophore-producing microbes. Similarly, observations during the fall reveal a peak in the abundance of siderophore BGCs at and below the DCM (Fig. 2C). This may reflect intensified iron recycling or the high demand for iron by the heterotrophic bacteria community as they respire sinking organic matter associated with the export pulse at Station ALOHA. The short residence times of iron at 300 m also suggest intense competition for iron at these depths. Finally, in the winter, siderophore concentrations and the presence of siderophore BGCs reduces significantly, likely reflecting the decrease in iron demand of heterotrophic bacteria as productivity and organic matter substrates diminish, or increased mixing that dilutes siderophore concentrations. This dataset provides compelling evidence that ligand production by the microbial community plays an important role in the seasonal cycling and retention of iron at Station ALOHA.

5. Acknowledgements

Special thanks to the Captain and crew of the R/V *Kilo Moana* and R/V *Ka'imikai-O-Kanaloa* for help with sample collection, and to Kendra A. Turk-Kubo for flow cytometry analyses. We would also like to thank Travis Mellett for helpful comments on the manuscript. RMB was funded by a Life Sciences-Simons Early Career Investigator in Marine Microbial Ecology and Evolution Awards (Award# 618401) and a Woods Hole Oceanographic Institution postdoctoral fellowship. LEM was funded by a Simons Postdoctoral Fellowship in Marine Microbial Ecology (Award #729162). MJC was funded by the Simons Collaboration on Ocean Processes (Award #721221).

Table 1. Siderophores measured in the water column and siderophore biosynthetic gene clusters (BGCs) identified at Station ALOHA. Siderophores identified in the water column are grouped according to type and are shown in the table based on that grouping. For example, multiple different forms of amphibactins were detected (Table S1) but are all grouped here under "amphibactins." Specific siderophore IDs can be found in Supplementary Table 1. The '+' denotes that the specific siderophore BGC was found in the 2015-2016 metagenomic dataset, while '-' indicates it was not detected.

Siderophore	Type	Biosynthetic Pathway	Depth(s)	Season	BGC in gene catalog
aerobactin	mixed	NIS	-	-	+
amphibactins	hydroxamate	NRPS	300-400	summer	-
anguibactin	catecholate	NRPS	-	-	+
enterobactin	catecholate	NRPS	-	-	+
ferrioxamaines	hydroxamate	NIS	15-400	spring, summer, winter	-
petrobactin	mixed	NIS/NRPS hybrid	15	winter	+
piscibactin	catecholate	NRPS	15	winter	+
(pseudo)alterobactin	catecholate	NRPS	15	winter	+
synechobactins	mixed	NRPS	15, 150	spring, summer, winter	-
vibrioferrin	carboxylate	NIS	15	winter	+
vibriobactin	catecholate	NRPS	-	-	+

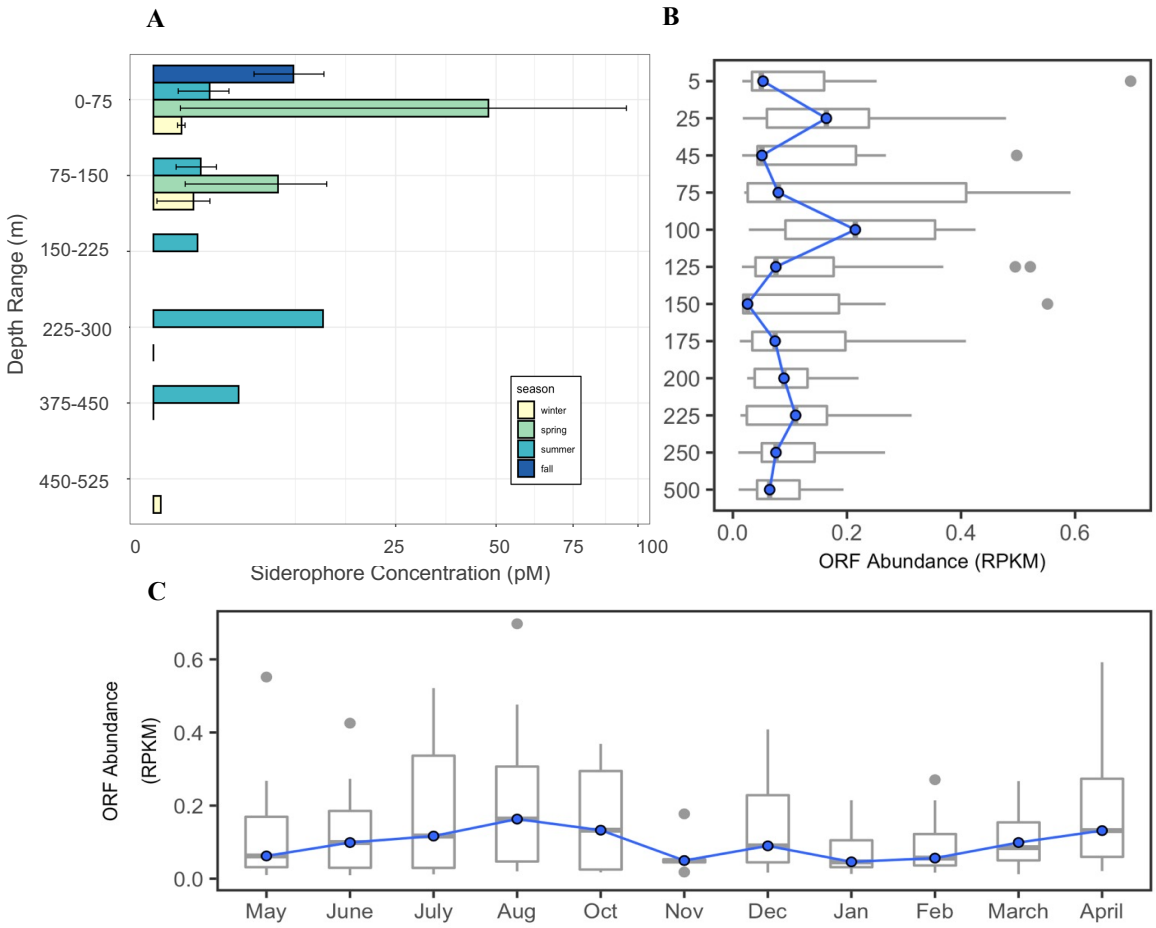

Figure 1. (A) Seasonal average dissolved siderophore concentrations collected at Station ALOHA. Error bars, when present, represent the standard error of samples collected in the same depth range in the same season. When no data is present for a given depth range and season, no samples were collected during that time. (B) Distribution across depth of the abundance of siderophore BGCs detected at Station ALOHA between May 2015 – April 2016. Blue points track the median ORF abundances at each depth and boxplots display quartile ranges of the total dataset at each depth with outliers plotted as distinct points. No data present between 250 – 500 m. (C) Monthly distributions of the abundance of siderophore BGCs detected at Station ALOHA between May 2015 – April 2016. Blue points track the median ORF abundances for each month and boxplots display quartile ranges of the total dataset for each month with outliers plotted as distinct points.

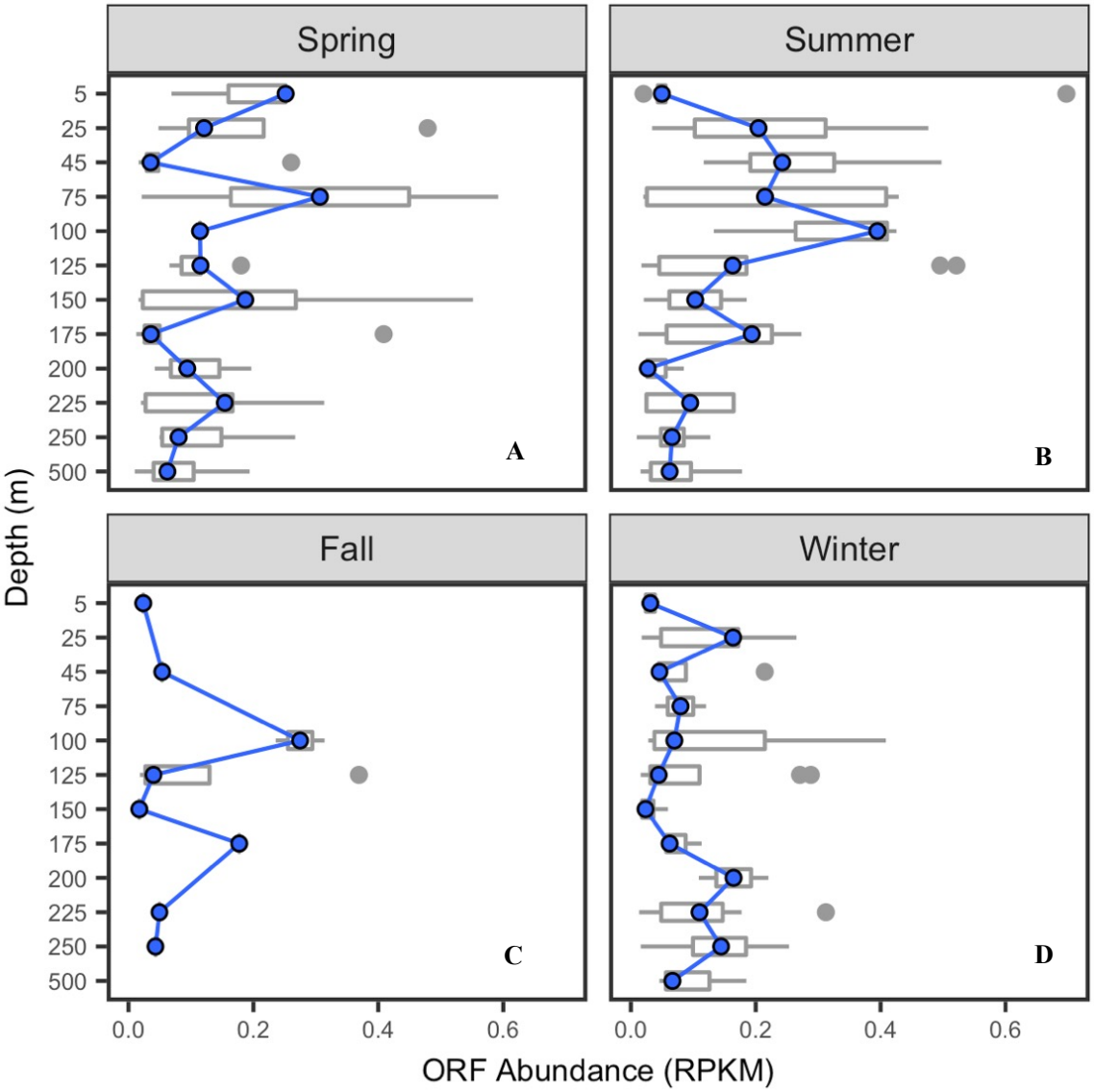

Figure 2. Distribution across seasons in spring (A), summer (B), fall (C) and winter (D) and with depth of siderophore BGCs detected at Station ALOHA between May 2015 – April 2016. Blue points track the median ORF abundances and boxplots display quartile ranges of the total dataset for each season at each depth with outliers plotted as distinct points. No data present between 250 – 500 m.

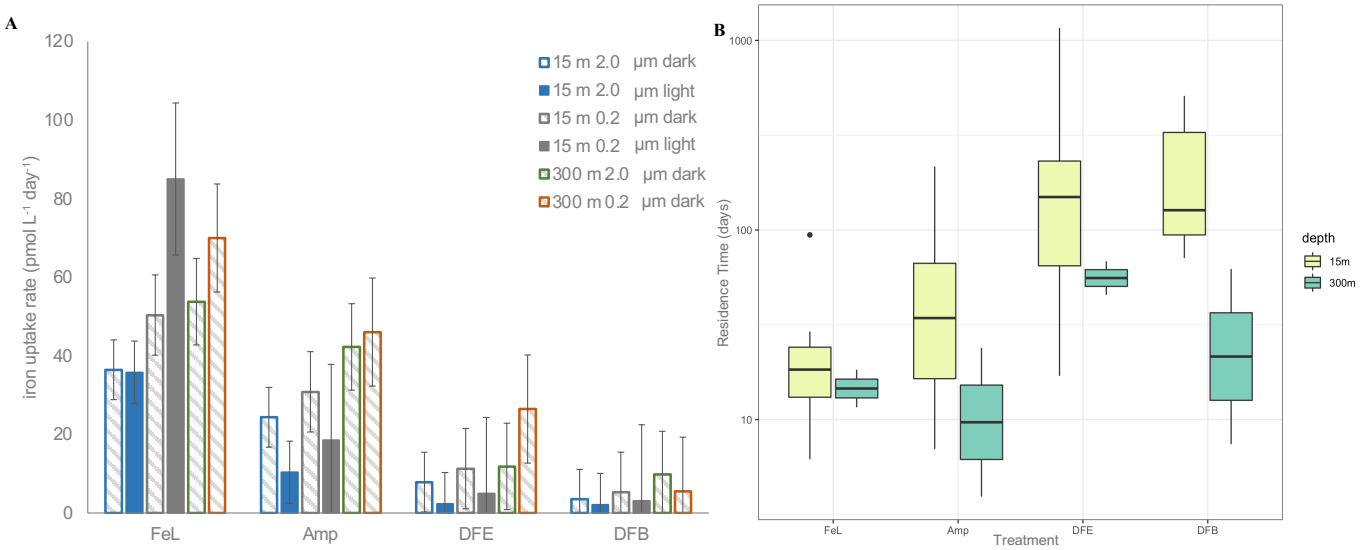

Figure 3. (A) Dissolved iron uptake rates in the surface (15 m) and upper mesopelagic (300 m) in the 2.0 µm and 0.2 µm size fraction (hatched bars) in the dark (grey shaded) and in the light. (B) Residence times of iron in the inorganic iron treatment (FeL), Fe-amphibactin treatment (Amp), ferrioxamine E treatment (DFE), and ferrioxamine B treatment (DFB) at 15 m (yellow) and 300 m (blue). Residence times at 300 m were statistically different from 15 m only in the DFB treatment (pairwise t-test, $p < 0.05$)

References

Barbeau, K. 2006. Photochemistry of organic iron(III) complexing ligands in oceanic systems. Photochem. Photobiol. **82**: 1505–1516. doi:10.1562/2006-06-16-ir-935

Boiteau, R. M., J. N. Fitzsimmons, D. J. Repeta, and E. A. Boyle. 2013. Detection of Iron Ligands in Seawater and Marine Cyanobacteria Cultures by High-Performance Liquid Chromatography-Inductively Coupled Plasma-Mass Spectrometry. Anal. Chem. **85**: 4357–4362. doi:10.1021/ac3034568

Boiteau, R. M., D. R. Mende, N. J. Hawco, and others. 2016. Siderophore-based microbial adaptations to iron scarcity across the eastern Pacific Ocean. Proc. Natl. Acad. Sci. **113**: 14237–14242.

Boiteau, R. M., C. P. Till, T. H. Coale, J. N. Fitzsimmons, K. W. Bruland, and D. J. Repeta. 2019. Patterns of iron and siderophore distributions across the California Current System. Limnol. Oceanogr. **64**: 376–389. doi:10.1002/lno.11046

Boyd, P. W., R. F. Strzepek, M. J. Ellwood, D. A. Hutchins, S. D. Nodder, B. S. Twining, and S. W. Wilhelm. 2015. Why are biotic iron pools uniform across high- and low-iron pelagic ecosystems? Global Biogeochem. Cycles **29**: 1028–1043. doi:10.1002/2014gb005014

Bundy, R. M., R. M. Boiteau, C. McLean, K. A. Turk-Kubo, M. R. McIlvin, M. A. Saito, B. A. S. Van Mooy, and D. J. Repeta. 2018. Distinct Siderophores Contribute to Iron Cycling in the Mesopelagic at Station ALOHA. Front. Mar. Sci. **5**: 1–15. doi:10.3389/fmars.2018.00061

Church, M. J., E. Kyi, R. O. Hall Jr, D. M. Karl, M. Lindh, A. Nelson, and E. K. Wear. 2021. Production and diversity of microorganisms associated with sinking particles in the subtropical North Pacific Ocean. Limnol. Oceanogr. **66**: 3255–3270.

Coale, T. H., M. Moosburner, A. Horák, M. Oborník, K. A. Barbeau, and A. E. Allen. 2019. Reduction-dependent siderophore assimilation in a model pennate diatom. Proc. Natl. Acad. Sci. U. S. A. **116**: 23609–23617. doi:10.1073/pnas.1907234116

Cordero, O. X., L.-A. Ventouras, E. F. DeLong, and M. F. Polz. 2012. Public good dynamics drive evolution of iron acquisition strategies in natural bacterioplankton populations. Proc. Natl. Acad. Sci. **109**: 20059–20064. doi:10.1073/pnas.1213344109

Eddy, S. R. 2011. Accelerated profile HMM searches. PLoS Comput. Biol. **7**: e1002195.

Fitzsimmons, J. N., and E. A. Boyle. 2014. Assessment and comparison of Anopore and cross flow filtration methods for the determination of dissolved iron size fractionation into soluble and colloidal phases in seawater. Limnol. Oceanogr. **12**: 246–263. doi:10.4319/lom.2014.12.246

Fitzsimmons, J. N., C. T. Hayes, S. N. Al-Subiai, R. Zhang, P. L. Morton, R. E. Weisend, F. Ascani, and E. A. Boyle. 2015. Daily to decadal variability of size-fractionated iron and iron-binding ligands at the Hawaii Ocean Time-series Station ALOHA. Geochim. Cosmochim. Acta **171**: 303–324.

Fontanez, K. M., J. M. Eppley, T. J. Samo, D. M. Karl, and E. F. DeLong. 2015. Microbial community structure and function on sinking particles in the North Pacific Subtropical Gyre. Front. Microbiol. **6**: 469.

Hawco, N. J., B. Barone, M. J. Church, and others. 2021. Iron depletion in the deep chlorophyll maximum: mesoscale eddies as natural iron fertilization experiments. Global Biogeochem. Cycles **35**: e2021GB007112.

Hawco, N. J., S.-C. Yang, P. Pinedo-González, E. E. Black, J. Kenyon, S. Ferrón, X. Bian, and S. G. John. 2022. Recycling of dissolved iron in the North Pacific Subtropical Gyre.

Limnol. Oceanogr. doi:https://doi.org/10.1002/lno.12212
Hayes, C. T., J. N. Fitzsimmons, E. A. Boyle, D. McGee, R. F. Anderson, R. Weisend, and P. L. Morton. 2015. Thorium isotopes tracing the iron cycle at the Hawaii Ocean Time-series Station ALOHA. Geochim. Cosmochim. Acta **169**: 1–16.
Hider, R. C., and X. Kong. 2010. Chemistry and biology of siderophores. Nat. Prod. Rep. **27**: 637–657. doi:10.1039/b906679a
Karl, D., R. Letelier, L. Tupas, and J. Dore. 1997. The role of nitrogen fixation in biogeochemical cycling in the subtropical North Pacific Ocean. Nature **388**: 533.
Karl, D. M., R. M. Letelier, R. R. Bidigare, K. M. Björkman, M. J. Church, J. E. Dore, and A. E. White. 2021. Seasonal-to-decadal scale variability in primary production and particulate matter export at Station ALOHA. Prog. Oceanogr. **195**: 102563.
Karl, D. M., and R. Lukas. 1996. The Hawaii Ocean Time-series (HOT) program: Background, rationale and field implementation. Deep Sea Res. Part II Top. Stud. Oceanogr. **43**: 129–156.
Kramer, J., Ö. Özkaya, and R. Kümmerli. 2020. Bacterial siderophores in community and host interactions. Nat. Rev. Microbiol. **18**: 152–163.
Letelier, R. M., K. M. Björkman, M. J. Church, and others. 2019. Climate-driven oscillation of phosphorus and iron limitation in the North Pacific Subtropical Gyre. Proc. Natl. Acad. Sci. U. S. A. **116**: 12720–12728. doi:10.1073/pnas.1900789116
Leu, A. O., J. M. Eppley, A. Burger, and E. F. DeLong. 2022. Diverse Genomic Traits Differentiate Sinking-Particle-Associated versus Free-Living Microbes throughout the Oligotrophic Open Ocean Water Column. MBio **13**: e0156922. doi:10.1128/mbio.01569-22
Li, H., and R. Durbin. 2009. Fast and accurate short read alignment with Burrows--Wheeler transform. bioinformatics **25**: 1754–1760.
Liao, Y., G. K. Smyth, and W. Shi. 2014. featureCounts: an efficient general purpose program for assigning sequence reads to genomic features. Bioinformatics **30**: 923–930.
Lis, H., Y. Shaked, C. Kranzler, N. Keren, and F. M. M. Morel. 2015. Iron bioavailability to phytoplankton: an empirical approach. ISME J. **9**: 1003–1013. doi:10.1038/ismej.2014.199
Longhurst, A. R. 2010. Ecological geography of the sea, Elsevier.
Luo, E., J. M. Eppley, A. E. Romano, D. R. Mende, and E. F. DeLong. 2020. Double-stranded DNA virioplankton dynamics and reproductive strategies in the oligotrophic open ocean water column. ISME J. **14**: 1304–1315. doi:10.1038/s41396-020-0604-8
Maldonado, M. T., and N. M. Price. 2001. Reduction and transport of organically bound iron by Thalassiosira oceanica (Bacillariophyceae). J. Phycol. **37**: 298–309. doi:10.1046/j.1529-8817.2001.037002298.x
Manck, L. E., J. Park, B. J. Tully, A. M. Poire, R. M. Bundy, C. L. Dupont, and K. A. Barbeau. 2022. Petrobactin, a siderophore produced by Alteromonas, mediates community iron acquisition in the global ocean. ISME J. **16**: 358–369.
Mawji, E., M. Gledhill, J. A. Milton, and others. 2008a. Hydroxamate Siderophores: Occurance and Importance in the Atlantic Ocean. Environ. Sci. Technol. **42**: 8675–8680.
Mawji, E., M. Gledhill, J. A. Milton, and others. 2008b. Hydroxamate Siderophores: Occurrence and Importance in the Atlantic Ocean. Environ. Sci. Technol. **42**: 8675–8680. doi:10.1021/es801884r
Mazzotta, M. G., M. R. McIlvin, and M. A. Saito. 2020. Characterization of the Fe metalloproteome of a ubiquitous marine heterotroph, Pseudoalteromonas (BB2-AT2): multiple bacterioferritin copies enable significant Fe storage†. Metallomics **12**: 654–667.

doi:10.1039/d0mt00034e
Medema, M. H., K. Blin, P. Cimermancic, and others. 2011. antiSMASH: rapid identification, annotation and analysis of secondary metabolite biosynthesis gene clusters in bacterial and fungal genome sequences. Nucleic Acids Res. **39**: W339--W346.
Mende, D. R., J. A. Bryant, F. O. Aylward, J. M. Eppley, T. Nielsen, D. M. Karl, and E. F. DeLong. 2017. Environmental drivers of a microbial genomic transition zone in the ocean's interior. Nat. Microbiol. **2**: 1367–1373. doi:10.1038/s41564-017-0008-3
Moore, L. E., M. I. Heller, K. A. Barbeau, J. W. Moffett, and R. M. Bundy. 2021. Organic complexation of iron by strong ligands and siderophores in the eastern tropical North Pacific oxygen deficient zone. Mar. Chem. **236**: 104021.
Pelve, E. A., K. M. Fontanez, and E. F. DeLong. 2017. Bacterial succession on sinking particles in the ocean's interior. Front. Microbiol. **8**: 2269.
Pinedo-González, P., N. J. Hawco, R. M. Bundy, and others. 2020. Anthropogenic Asian aerosols provide Fe to the North Pacific Ocean. Proc. Natl. Acad. Sci. U. S. A. **117**: 27862–27868. doi:10.1073/pnas.2010315117
Poff, K. E., A. O. Leu, J. M. Eppley, D. M. Karl, and E. F. DeLong. 2021. Microbial dynamics of elevated carbon flux in the open ocean's abyss. Proc. Natl. Acad. Sci. **118**: e2018269118.
Saito, M. A., M. R. McIlvin, D. M. Moran, and others. 2020. Abundant nitrite-oxidizing metalloenzymes in the mesopelagic zone of the tropical Pacific Ocean. Nat. Geosci. **13**: 355–362.
Salmon, T. P., A. L. Rose, B. A. Neilan, and T. D. Waite. 2006. The FeL model of iron acquisition: Nondissociative reduction of ferric complexes in the marine environment. Limnol. Oceanogr. **51**: 1744–1754.
Sandy, M., and A. Butler. 2009. Microbial iron acquisition: marine and terrestrial siderophores. Chem. Rev. **109**: 4580–4595.
Shaked, Y., and H. Lis. 2012. Disassembling iron availability to phytoplankton. Front. Microbiol. **3**: 123. doi:10.3389/fmicb.2012.00123
Strzepek, R. F., M. T. Maldonado, J. L. Higgins, J. Hall, K. Safi, S. W. Wilhelm, and P. W. Boyd. 2005. Spinning the "ferrous wheel": The importance of the microbial community in an iron budget during the FeCycle experiment. Global Biogeochem. Cycles **19**. doi:10.1029/2005GB002490
Tortell, P. D., M. T. Maldonado, and N. M. Price. 1996. The role of heterotrophic bacteria in iron-limited ocean ecosystems. Lett. to Nat. **383**: 330–332.
Tovar-Sanchez, a. 2003. A trace metal clean reagent to remove surface-bound iron from marine phytoplankton. Mar. Chem. **82**: 91–99. doi:10.1016/S0304-4203(03)00054-9
Vraspir, J. M., and A. Butler. 2009. Chemistry of Marine Ligands and Siderophores. Ann. Rev. Mar. Sci. **1**: 43–63. doi:10.1146/annurev.marine.010908.163712
Watson, S. W., and M. Mandel. 1971. Comparison of the morphology and deoxyribonucleic acid composition of 27 strains of nitrifying bacteria. J. Bacteriol. **107**: 563–569.